

Generalized Kitaev Spin Liquid model and Emergent Twist Defect

Bowen Yan ^{*1} and Shawn X. Cui ^{*1,2}

¹Department of Physics and Astronomy, Purdue University, West Lafayette

²Department of Mathematics, Purdue University, West Lafayette

{yan312, cui177} @purdue.edu

Abstract

The Kitaev spin liquid model on honeycomb lattice offers an intriguing feature that encapsulates both Abelian and non-Abelian anyons. Recent studies suggest that the comprehensive phase diagram of possible generalized Kitaev model largely depends on the specific details of the discrete lattice, which somewhat deviates from the traditional understanding of "topological" phases. In this paper, we propose an adapted version of the Kitaev spin liquid model on arbitrary planar lattices. Our revised model recovers the toric code model under certain parameter selections within the Hamiltonian terms. Our research indicates that changes in parameters can initiate the emergence of holes, domain walls, or twist defects. Notably, the twist defect, which presents as a lattice dislocation defect, exhibits non-Abelian braiding statistics upon tuning the coefficients of the Hamiltonian on a standard translationally invariant lattice. Additionally, we illustrate that the creation, movement, and fusion of these defects can be accomplished through natural time evolution by linearly interpolating the static Hamiltonian. These defects demonstrate the Ising anyon fusion rule as anticipated. Our findings hint at possible implementation in actual physical materials owing to a more realistically achievable two-body interaction.

1 Introduction

Since Kitaev proposed the Kitaev Quantum Double model[1], it has garnered considerable attention due to its typical anyon behavior and the paradigm it provides for topological quantum computation. The model demonstrates how one can circumvent local errors by encoding information into anyon types and executing gates through anyon braiding. Anyon theory is comprehensively described by Unitary Modular Tensor Categories (UMTC), and it has been proven

^{*}Corresponding author

that certain non-Abelian cases, such as Fibonacci Anyon, can support universal quantum computation.

Following this development, numerous lattice models have been proposed with the objective of identifying different types of anyons. Two significant classes of these include the Kitaev Quantum Double model[1] and the Levin-Wen model[2]. These models actualize anyon models from varying perspectives, which are described by the Drinfeld center of a fusion category.

The realization of the actual topological phase is a complex and pivotal task. Renowned models, such as the Kitaev Quantum Double model and Levin-Wen model, necessitate multi-body interactions, making them challenging to implement in a real-world laboratory setting. While some comparatively achievable cases, such as the toric code, are not suitable for universal computation because it only supports Abelian anyons. This reality has led to an increased interest in the twist defect, as introduced by [3]. This defect exemplifies a non-Abelian Ising anyon, which stems from the lattice dislocation of the abelian anyon case, the toric code model. Recent experimental observations of the Ising anyon statistics, as reported by [4], attest to this. It should be noted that the defect is dependent on the disruption of the lattice's local two-colorability.

Another intriguing model is the Kitaev spin liquid Model[5], which supports Abelian anyons in the gapped phase region, as well as non-Abelian anyons upon the introduction of a magnetic field to the gapless phase. This model is simple yet fruitful. But the definition of the model relies heavily on the geometry of honeycomb lattice, which deviates the idea of topological phase and is the main question to be solved in this paper. Moreover, it also has been pointed out that a spin liquid model on honeycomb lattice with lattice dislocation will generate the twist defect as in [6]. The generalization to Zetor model has been shown in [7]. This model is potentially easily realizable in a real laboratory due to the two-body nearest interaction.

Considerable theoretical progress has been made in the generalization of this model. Examples include those on a translationally invariant two dimensional lattice with higher-coordination vertices [8][9][10], on a two-dimensional amorphous lattice [11], a three-dimensional diamond lattice [12], and works on trivalent 3D lattices [13]. It is clear that the overall phase diagram is strongly influenced by the geometric specifics of the lattice, thus also deviating our traditional understanding of 'topological' phases.

In this paper, we demonstrate that the entire theory can be formulated on a generic planar lattice. The main motivation relies on the toric code limit of the original honeycomb spin liquid model as mentioned before, which is briefly reviewed in section(2). We sketch the main idea here and details are in the following sections.

The Hamiltonian of the honeycomb spin liquid system is a summation of weighted check operators, which are two-body nearest Pauli operators. The Hamiltonian is frustrated due to non-commutation of the check operators. We say a check operator in the Hamiltonian is dominant if the coefficient of the operator is much larger than others. Kitaev selected what he refers to as 'z-link' check operators to take dominance in the Hamiltonian. As a result, the vicinity

of the ground state in the spectrum can be accurately described by a toric code model. The actual choice of 'z-link' check operators is not important. The key fact is that 'z-link' check operators composite a maximum set of commuting operators, which is denoted as stabilizer center S_c in this paper. S_c satisfies that any check operator outside this set should anticommutes with exactly two elements in S_c . So our method is to find a way to define check operators on arbitrary planar lattice and then find a proper S_c . We prove that will recover a toric code model at the vicinity of the ground state if all elements in S_c are dominant as the Hamiltonian is the summation of all parameterized check operators.

Moreover, we find one interesting phenomenon that we get toric code with defects if we slight break the requirement of S_c . Further, we propose that a linear interpolating Hamiltonians, which statically has different dominant S_c s, could be a natural way to create, move, and fuse defects in a physical system. This approach circumvents the need for geometric deformation or the application of a coding method. This proposal might inspire real material realization since we only need to establish and adjust the strength of two-body interactions, as illustrated in section 3.4. Moreover, a circuit description is plausible since these operations are facilitated by time evolution operators.

This paper is organized as follows:

In Section 2, we provide a concise review of the original honeycomb model and reintroduce necessary notations.

Section 3 introduces our method of generalization. Initially, we rewrite the toric code on a lattice where qubits are positioned on vertices instead of edges, as discussed in Section 3.1. This rewriting is pretty important since the recovery of toric code from the generalized spin liquid model is naturally on a lattice where qubits are placed on vertices. Subsequently, in Sections 3.2 and 3.3, we demonstrate that, given an appropriate choice of a Stabilizer Center (S_c), the toric code can be recovered when the shrunken lattice is 2-colorable. We should note that a local disruption of the two-colorability of the shrunken lattice leads to the emergence of a twist defect, which manifests itself as an Ising Anyon.

Section 3.4 illustrates the process of creation, movement, and fusion of defects through time evolution operators, indicating that all these processes can be facilitated by unitary operators.

Next, in Section 3.5, we demonstrate that the entire model can be treated as a zero-logic-qubit subsystem code.

Finally, Section 4 concludes the paper and discusses potential future extensions.

2 Kitaev Honeycomb Model

Let us briefly revisit the Kitaev Honeycomb Model and establish some notations. The lattice, depicted in Figure 1a and denoted by $\Gamma = (V, E, P)$, consists of vertices (V), edges (E), and faces (P).

The notation $\partial_1 e$, $\partial_2 e$ is used to refer to the two vertices at the end of

edge $e \in E$, and $\partial e = \{\partial_1 e, \partial_2 e\}$ indicates the set of these vertices. $N(A)$ is the count of the set A . A frequently used symbol d_v denotes the count of set $e|e \in E, v \in \partial e$, i.e., the degree of the vertex v . $Bo(p) \subseteq E$, for $p \in P$ represents the edges that border the plaquette p .

Each vertex houses a qubit. The total Hilbert Space is:

$$\mathcal{H} := \bigotimes_{e \in E} \mathcal{H}_e \quad (1)$$

Each edge on the lattice is associated with a symbol X, Y, Z . For the honeycomb lattice, we label all the edges as illustrated in Figure 1a, consistent with the original paper[5]. These edges are referred to as "x-edges", "y-edges", and "z-edges". The edge associated with $x(y, z)$ involves a two-body action $X \otimes X(Y \otimes Y, Z \otimes Z)$ on the qubits at both ends of the edge. The operators linked to edges are defined as check operators. In this paper, we use X, Y, Z to represent Pauli Operators.

The Hamiltonian is the summation of weighted check operators:

$$H = -J_x \sum_{x\text{-edges}} X \otimes X - J_y \sum_{y\text{-edges}} Y \otimes Y - J_z \sum_{Z\text{-edges}} Z \otimes Z \quad (2)$$

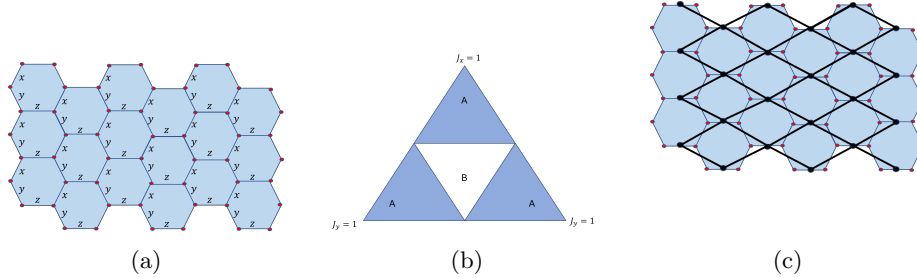


Figure 1: (a) Figure 1: The original Honeycomb Lattice.(b) Figure 2: Phase diagram depicting the gapped phases when one of J_x , J_y , or J_z is dominant. The dominance of these terms results in a phase that is mathematically equivalent to a toric code model.(c) Figure 3: Depiction of the mapping process when J_z is dominant, showing how the two physical qubits are reduced to one effective qubit in the ground state of the P_z terms.

As depicted in Figure 1b, the phase diagram of the Honeycomb model is well-defined. In the $A(B)$ region, it represents a gapped(gapless) phase. Kitaev explicitly demonstrated, using perturbation theory, that the gapped phase is the toric code phase, where one of the J_x, J_y, J_z variables is much larger than others, or equivalently saying one set of check operators of $x\text{-edges}, y\text{-edges}, z\text{-edges}$ is dominant.

Looking at the vicinity of the ground state when J_z is dominant. The two qubits connected by $z\text{-edges}$ will stay at the ground state of the the check

operator $Z \otimes Z$. We say these two qubits are effectively "shrunk" to a single qubit. Subsequently, the lattice is also shrunk by replacing the edge with its end vertices to be a single vertex, as shown in Figure 1c. This is referred to as the "shrunk" lattice at z -edges".

Let's rephrase this in our terms. We denote these check operators associated with z -edges as a Stabilizer center S_c . We obtain a shrunk lattice at this S_c . The ground state under this limit is two-folded: it is simultaneously the ground state of S_c and the ground state of all plaquette terms W_p . Where W_p is the product of check operators associated to edges in $Bo(p)$.

Generally, on a trivalent lattice, a Hamiltonian of the following form can be considered:

$$H = - \sum_{e \in E} J_e P_e \quad (3)$$

The check operator P_e is defined in a similar fashion as above; it is a tensor product of Pauli operators acting on the qubits situated at the end of edge e . We state that two check operators are unconnected if the edges associated with these operators are not connected. The crucial feature is to maintain the following commutative relation:

$$[P_e, P_{e'}] = 0 \text{ if } \partial e \cap \partial e' = \emptyset \quad (4)$$

$$\{P_e, P_{e'}\} = 0 \text{ if } \partial e \cap \partial e' \neq \emptyset \quad (5)$$

$$(6)$$

For any $e \neq e'$. This means that check operators should anticommute if they intersect at one vertex and commute in other scenarios. We require all check operators in S_c to be unconnected. When we allow S_c to be dominant, we obtain a shrunk lattice by replacing the edges of S_c with a single vertex. We will demonstrate that this will be a specific surface code. Indeed, for a general lattice, the shrunk lattice at different S_c will vary. While in this case, the shrunk lattice at x -edges or z -edges are all square lattices. In [14], their shrunk lattice is a kagome lattice (when the qubits are considered to be placed on vertices). We will frequently utilize the concept of a shrunk lattice at a given S_c .

3 Generalized Method

3.1 Toric Code on a lattice where qubits are placed on vertices

The toric code model is defined on an arbitrary planar lattice $\Gamma = (V, E, P)$, with one qubit placed on each edge. The Hamiltonian is:

$$H = - \sum_v A_v - \sum_p B_p \quad (7)$$

Here, $A_v = \bigotimes_{e|v \in \partial e} X_e$ and similarly, $B_p = \bigotimes_{e|e \in Bo(p)} Z_e$. The symbols X_e and Z_e indicate that the Pauli operator X and Z acts on the qubit placed on the edge e . For our purposes, we need to reshape the lattice into a more convenient form as shown in figure 2. The process is as follows. First, we attach a new vertex on each edge, denoted by red dots. We add one edge to connect edges e_1 and e_2 if they satisfy

$$e_1 \neq e_2 \quad (8)$$

$$N(\partial e_1 \cap \partial e_2) = 1 \quad (9)$$

$$\exists p \in P, e_1, e_2 \subseteq Bo(p) \quad (10)$$

We will add two edges to connect e_1 and e_2 if $N(\partial e_1 \cap \partial e_2) = 2$ in the above requirement. This results in a new lattice $\Gamma' = (V', E', P')$, where V' is the set of red dots and $V' = E$ as sets. E' is the set of newly added edges connecting red dots and $P' = V \cup P$ as sets.

Notably, the degree of the new vertex is automatically 4. The new plaquettes are two-colored by vertices and plaquettes of Γ . Consequently, the toric code becomes a lattice model on Γ' , with one qubit placed on each vertex. In the new lattice as in figure 2c, the plaquette $p_g(p_r)$ with a green(red) circle has a plaquette term that is $\bigotimes X(Z)$ on each qubit on the boundary of $p_g(p_r)$, corresponding to previous $A_v(B_p)$ operators.

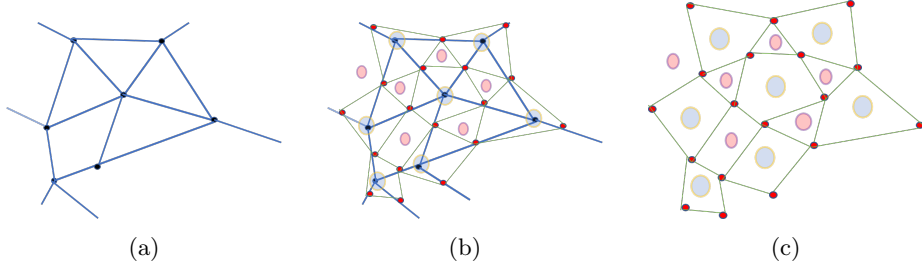


Figure 2: (a) Figure 1: Original lattice model with qubits placed on edges. Black dots represent vertices of the lattice. (b) Figure 2: Transformation process of the lattice. Red dots label the center of edges. Two red dots are connected if they belong to the same plaquette and are simultaneously connected to a single vertex. New plaquettes are colored in red and grey circles. (c) Figure 3: Final lattice model with qubits on vertices. The original lattice is removed. A_v and B_p operators act individually on the two types of plaquettes, labeled by red and grey circles respectively.

3.2 Generalized model on a lattice with all vertices having even degree

Now, we are prepared to generalize the Kitaev Spin Liquid Model. We begin with a lattice $\Gamma = (V, E, P)$, where each vertex $v \in V$ has an even degree d_v .

We place $d_v/2 - 1$ qubits on each vertex. For k qubits, we can define $2k + 1$ mutually anti-commuting Clifford operators as follows:

$$\begin{aligned}
p_1 &= 1 \otimes 1 \otimes 1 \otimes \cdots X \\
p_2 &= 1 \otimes 1 \otimes 1 \otimes \cdots Y \\
&\vdots \\
p_{2t+1} &= \underbrace{1 \cdots 1}_{k-t-1} \otimes X \otimes Z \otimes \cdots Z \\
p_{2t+2} &= \underbrace{1 \cdots 1}_{k-t-1} \otimes Y \otimes Z \otimes \cdots Z \\
&\vdots \\
P_{2k+1} &= Z \otimes Z \otimes Z \otimes \cdots Z
\end{aligned} \tag{11}$$

Importantly, because we will finally reach at toric code, the signs of each term do not significantly matter (different sign configurations are related by unitary transformations). This means we can consider each operator in the Pauli group $\mathcal{P} = \{G/\{+1, -1, +i, -i\}\}$. Here G is denoted to represent the set of all possible tensor product of Pauli operators, for avoiding abusing notation.

Within the Pauli group, the phase gate P_{gate} interchanges X and Y , while Z is not affected, which can swap P_{2t+1} with P_{2t+2} for any $0 \leq t < k$. Subsequently, the Hadamard gate H_{gate} flips X and Z , which in turn flips P_{2k+1} and P_{2k-1} . The gate $S_{gate} = P_{gate} \circ H_{gate} \circ P_{gate}$ flips Y and Z . Then, a sequence of conjugations flips P_1 with P_4 . It's worth noting that it's sufficient to consider only the last two qubits. Here's how to flip $X \otimes Z$ with $1 \otimes Y$, without changing the other operators:

$$\begin{array}{ccccccc}
X \otimes Z & \xrightarrow{H_{gate} \otimes \text{Id}} & Z \otimes Z & \xrightarrow{\text{CNOT}} & 1 \otimes Z & \xrightarrow{S_{gate} \otimes S_{gate}} & 1 \otimes Y \xrightarrow{P_{gate} \otimes 1} 1 \otimes Y \\
1 \otimes Y & \xrightarrow{H_{gate} \otimes \text{Id}} & 1 \otimes Y & \xrightarrow{\text{CNOT}} & Z \otimes Y & \xrightarrow{S_{gate} \otimes S_{gate}} & Y \otimes Z \xrightarrow{P_{gate} \otimes 1} X \otimes Z
\end{array}$$

This is sufficient to exchange any P_i with P_j by stacking the aforementioned operations, implying that any operator distribution is equivalent. Let us look at a lattice with all vertices that have degree four first. As shown in diagram 3, for each vertex, we distribute P_1 to P_4 to the end of edge that is connected to the vertex, and P_5 to the vertex itself. An operator P_e is associated with an edge e , which is the tensor product of operators from the two ends. An operator P_v associates with a vertex v , which is P_5 . The Hamiltonian is as follows:

$$H = - \sum_v J_v P_v - \sum_e J_e P_e \tag{12}$$

$$P_e = P_{\partial_1 e} \otimes P_{\partial_2 e} \tag{13}$$

Now let J_v dominate. Note that these operators commute with each other, so they share common eigenspaces. Let $J_e \ll J_v$, $J_v = 1$ and examine the corresponding perturbation theory where $H_0 = \sum_v P_v$ and $V = \lambda \sum_e J_e P_e$. λ

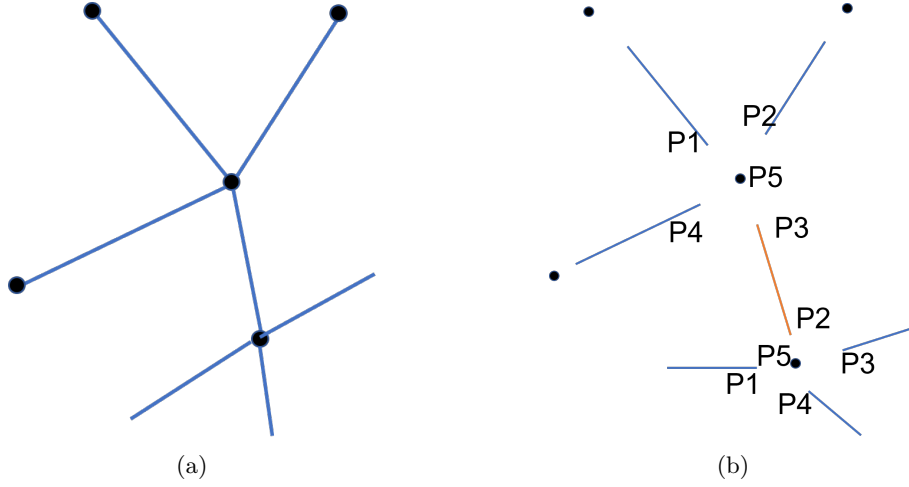


Figure 3: (a) Figure 1: A local part of the entire lattice diagram. This focuses on the interactions occurring at a specific vertex and the surrounding edges.(b) Figure 2: A simplified illustration for convenience, showing the assignment of operator P_1 through P_4 from each vertex v to the surrounding edges, while P_5 is assigned to the vertex v itself, denoted to be P_v . Notably, the operator on the orange edge is $(1 \otimes X) \otimes (Y \otimes Z)$, or simply $P_3 \otimes P_2$.

is a small factor to indicate the perturbation order. Denote $|GS\rangle$ as the ground state of H_0 . As in Kitaev's paper [5], the effective Hamiltonian around the ground state is given by:

$$H_{eff} = T(V + VG'_0V + VG'_0VG'_0V + \dots)T \quad (14)$$

Where, $T = |GS\rangle\langle GS|$ is the projector onto the ground state of P_v s, and $G'_0 = (1/(E_0 - H_0))'$, where the prime notation implies G'_0 vanishes on the ground state and acts normally on the excited states.

We could conclude from appendixA, the effective Hamiltonian is:

$$H_{eff} = \sum_p \alpha_{l_p} \lambda^{l_p} W_p + constant \quad (15)$$

l_p represents the number of elements in $Bo(p)$, equivalent to the count of edges bordering the plaquette. W_p is the plaquette operator, which is the product of check operators boarding the plaquette.

Notice, when P_v is dominant, the two qubits placed on the vertex is effectively one qubit. So our stabilizer center S_c is equal to the set of P_v s and the shrunk lattice is exactly the same as before. The shrunk lattice has $d_v = 4$, and the action of plaquette terms W_p around each vertex, as illustrated in figure4a, exert the same local action on the vertex of the toric code case as shown in3.1.

The remaining task is to illustrate the case of $d_v = 2k, k > 2$, where k is an integer. Generally, for a vertex with an even d_v , we place $k = d_v - 1$ qubits on

the vertex, and designate $\bigotimes_k Z$, or $P_{d_{2k+1}}$ to be P_v and distribute the remaining d_v Clifford operators to the surrounding edges. The check operator is defined as in case where $d_v = 4$. Then the phase we are investigating is when all P_v s are dominant. We illustrate the example of a vertex with $d_v = 6$ as in diagram4b. The computation is grounded on the mapping table to find the effective Hamiltonian as in1. Essentially, we give a specific distribution of operators around the vertex. And calculate the effective action of the plaquette terms on this vertex, we observe that the effective two qubits split to two connected vertices with $d_v = 4$. It's clear both vertices maintain consistent and identical local properties as of toric code. The generic mapping table for vertex with degree $d_v \geq 4$ is shown in appendix B when we look at the ground state of dominant P_v s, each vertex with degree $d_v = 2k$ will split to $k - 1$ vertices with degree 4 .

Operator	Effective operator
$X \otimes X \otimes 1$	$X \otimes 1$
$1 \otimes X \otimes X$	$1 \otimes X$
$1 \otimes 1 \otimes Z$	$1 \otimes Z$
$1 \otimes Z \otimes 1$	$Z \otimes Z$
$Z \otimes 1 \otimes 1$	$Z \otimes 1$

Table 1: Mapping Table for a vertex with $d_v = 6$

Here, we call the transformation from $d_v = 2k$ to connected $k - 1$ degree 4 vertices the shrunk lattice component. After splitting all $d_v = 2k$ vertices, we get the shrunk lattice. We could conclude we could recover a toric code phase in the generalized Kitaev Model when the shrunk lattice is two-colorable.

Remark 2: One may worry about some unfortunate occasion that $\alpha_{l_p} = 0$, it is a path-dependent factor and depends heavily on the details of the lattice and the choice of S_c . But we argue a method to potentially fix it. We would say, for a zero α_{l_p} which have multiple channel in the diagram12, we can probably find a nonzero $\alpha_{l_{p+2}}$ by insert a pair of P_{e_0} in the process to build up W_p , where $e_0 \notin Bo(p)$ into the digram, which will change the action of G'_0 between the pair of P_{e_0} . Since the action is generally non-linear, if it's still zero, we could insert more. Finally W_p may survive in higher order of perturbation theory.

Remark 3: if there is huge plaquette in the lattice Γ , since l_p is large, λ^{l_p} is generally so small that this plaquette could be treated as a hole or a boundary, of which the type depends on the color of it. Or, if some $\alpha_{l_p} = 0$, and couldn't survive as in remark 1, or it only survive in really high order perturbation, it also serves as a hole in the toric code model. (Notice, toric code model is self-dual, so the type does not really matter)

3.3 Generalized model on arbitrary planar lattice

So The remaining question is how to deal with vertex with odd $d_v \geq 5$. It's not surprising to place $(d_v - 1)/2$ qubits on the edge. And distribute d_v Clifford

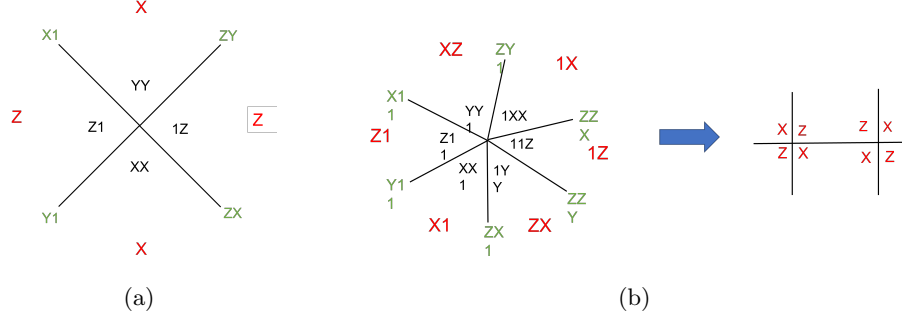


Figure 4: (a) Figure 1: This illustration demonstrates how the effective plaquette terms are obtained on the ground state of the P_e s. The green operator represents one of the anticommuting Clifford operators associated with edges. The black operator illustrates the plaquette term on a given vertex, and the red operator presents the effective plaquette term on the same vertex. (b) Figure 2: This depiction also shows how a vertex with degree $d_v = 6$ is transformed into two connected vertices, each with a degree of $d_v = 4$. It is essential to note that the effective action is consistent with the toric code case.

operators to surrounding edges. Then we already could conclude the general definition on general lattice $\Gamma = (V, E, P)$ that:

$$H = - \sum_{v|d_v \text{ is even}} J_v P_v - \sum_{e \in E} J_e P_e \quad (16)$$

$$P_e = P_{\partial_1 e} \otimes P_{\partial_2 e} \quad (17)$$

Then we pick the stabilizer center S_c which contains all $P_v|v \in V$ and a subset S_e of $P_e|e \in E$ satisfying that any two $P_e \in S$ commute with each other and commute with $P_v|v \in V$. That is to say that S_e are check operators on the edges that connect vertices with odd d_v . If we further require the shrunk lattice at S_c is a two-colorable degree-4 lattice, or equivalently, any two vertices with odd degree was shrunk. Then the effective Hamiltonian is the toric code Model when the coefficients of S_c are dominant. The proof involves transferring the lattice to a lattice where all vertices have even degrees. Notice that if we let the operator on the edge connecting two vertices with odd degree d_1 and d_2 dominant, it is equivalent to a vertex with degree $d_1 + d_2 - 2$ with dominant P_v , as shown in figure 5. So we could conclude, on general lattice Γ , if there exists a set of S_c , that all vertices get shrunk and the shrunk lattice is 2-colorable. The generalized Kitaev Spin liquid model resides in a toric code phase.

3.4 Emergent Twist Defect in the gapped phase

In all previous instances, we selected S_c such that any check operator would violate two terms in S_c , and all vertices with odd degrees being paired with

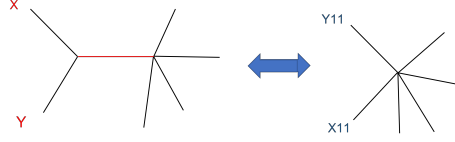


Figure 5: This illustration demonstrates that a vertex of degree 3 combined with a vertex of degree 5 is equivalent to a single vertex of degree 6. Here, equivalence means that they have same effective surrounding plaquette terms.

each other. What happens if there is an odd degree vertex, for example a trivalent vertex, that has not been paired with another odd degree vertex? Let us look back at the Honeycomb lattice again, as depicted in figure 7b, the effective Hamiltonian is a toric code model with two defects, similarly as in [3]. Notice in our case, there is one more plaquette as well as one more qubit. It shows that we can create dislocation defect at the toric code level with a regular lattice at the spin liquid level! As studied in [15], this type of lattice dislocation defect could capture unpaired Majorana modes in the original Honeycomb model.

Let's calculate α_{l_p} for these different plaquettes explicitly. For a standard square, $\alpha_4 = -1/16$, while for a pentagonal plaquette, $\alpha_5 = -3/32$. The calculation of the parallelogram between the two defects mirrors the situation as a regular square in the Kitaev Honeycomb case, so it also yields a non-zero result. The defect emerges as an Ising anyon exhibiting non-Abelian statistics, as experimentally observed by [4].

It's important to note that the lattice itself is regular and the lattice dislocation at the toric code level is due to a specific choice of S_c ! Remarkably, altering S_c is simpler than deforming the lattice itself. We will demonstrate in the following that a linearly interpolating Hamiltonian with different S_c choices can manipulate the defects.

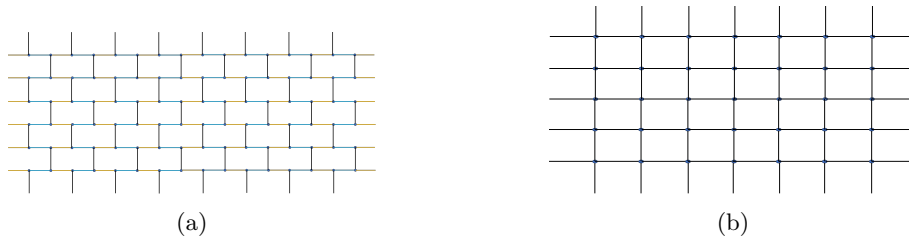


Figure 6: (a) Shows a honeycomb lattice where all vertices have been paired and shrunk by dominating the yellow edges. (b) The resulting effective or shrunk lattice where a toric code Hamiltonian acts.

The defect stays on the a remaining trivalent vertex, since the degree three will break the local 2-colorability, as marked in figure 7a, so moving defect is to move the remaining trivalent vertex.

Let us look at figure 8, a part of a large lattice as in figure 6 or in figure 7.

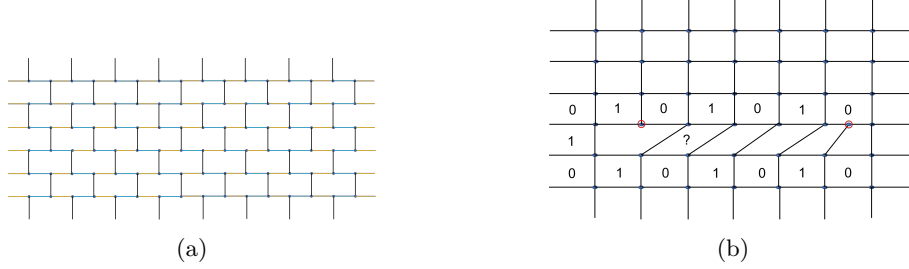
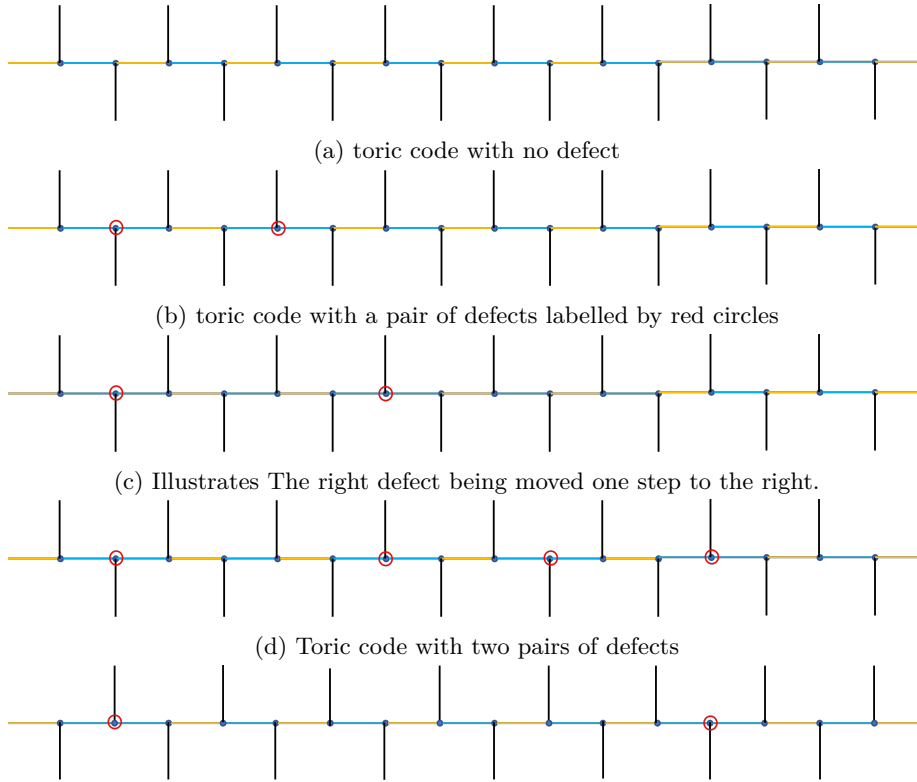


Figure 7: (a) Displays a situation where two trivalent vertices (labelled by red circles) are not shrunk with another vertex. (b) shows the underlined phase where all check operators on yellow edges are dominant. This represents the toric code with a pair of defects.



(e) Illustrates the process of fusing the two middle defects, which merges the separate pairs into a single pair.

Figure 8: The figures presented above depict the static Hamiltonian on a portion of the lattice. It is required that all check operators on yellow edges be dominant. These check operators will lead to varying cases of the effective toric code Hamiltonian, with or without defects.

All check operators on yellow edges are set to be dominant. Everything outside of this local part is the same. It shows five possible configurations, the effective Hamiltonian would be toric code with or without defects. We introduce time evolution to achieve the transformation between these static states, which is to create, move and fuse defects.

Let us take the movement of the defect as a detailed example. The rest is similar. Consider a more detailed local structure in figure 9, which is the transformation from 8b to 8c, we use $H(0)$ and $H(T)$ to represent their corresponding static Hamiltonian. We introduce the linear interpolating between them

$$H(t) = H(0)(1 - \frac{t}{T}) + H(T)\frac{t}{T} \quad (18)$$

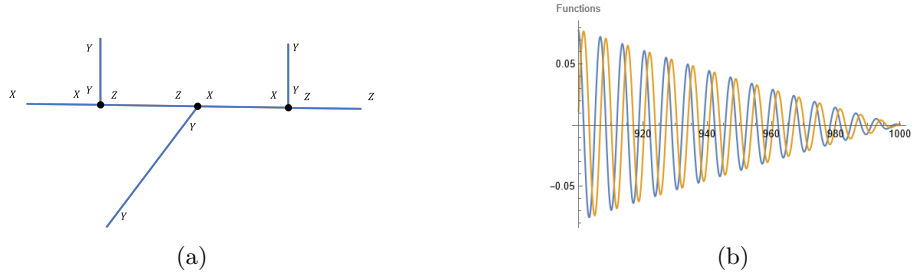


Figure 9: The figure on the left above depicts a detailed local section to address the movement of a defect, with the check operator explicitly labeled. On the right, the numerical result is displayed, illustrating that the real and imaginary differences between β_1 and β_2 vanish at $T = 1000$. Furthermore, this pattern holds true for all $T > 1000$.

Note that most terms remain unchanged, contributing to a phase term through their time-independent coefficients, as the state is always their eigenstate with an eigenvalue of +1. The only non-trivial one is:

$$H = -\frac{t}{T}Z \otimes Z \otimes 1 + -(1 - \frac{t}{T})1 \otimes X \otimes X \quad (19)$$

The time evolution operator(TEO):

$$O(t) = \mathcal{T} \int e^{iH} dt \quad (20)$$

This is a formal notation; calculations need to be done by explicitly applying the Time Order operator \mathcal{T} . But we realize that after expanding $O(t)$, the general form is:

$$O(t) = a(t) + b(t)Z \otimes Z \otimes 1 + c(t)1 \otimes X \otimes X + d(t)Z \otimes Y \otimes X \quad (21)$$

Where a, b, c, d are complex, time dependent functions. Notice, this operator $O(t)$ acts on the ground state of $1 \otimes X \otimes X$, so we could use a simpler form

that since $1 \otimes X \otimes X$ has trivial action:

$$O(t) = \beta_1 + \beta_2 Z \otimes Z \otimes 1 \quad (22)$$

By using

$$\frac{dO(t)}{dt} = HO(t) \quad (23)$$

We numerically solve $O(t)$ and find that $O(T) = \beta(1 + Z \otimes Z \otimes 1)$. β is some unimportant complex number that depends on T . At $t = 0$, the three qubits have two effective qubits with following basis.

$$|00\rangle_{t=0} = |0\rangle(|00\rangle + |01\rangle + |10\rangle + |11\rangle) \quad (24)$$

$$|01\rangle_{t=0} = |0\rangle(|00\rangle - |01\rangle - |10\rangle + |11\rangle) \quad (25)$$

$$|10\rangle_{t=0} = |1\rangle(|00\rangle + |01\rangle + |10\rangle + |11\rangle) \quad (26)$$

$$|00\rangle_{t=0} = |1\rangle(-|00\rangle + |01\rangle + |10\rangle - |11\rangle) \quad (27)$$

$$(28)$$

The basis chosen is to keep the action of the surrounding unperturbed plaquette terms unchanged. Since the ground state remains:

$$|GS\rangle_{t=0} = \prod_{p \in P} \frac{W_p + 1}{2} \bigotimes_{v' \in V'} |0\rangle_{v'} \quad (29)$$

Where V' is the vertex set of the shrunk lattice. And the $|0\rangle_{v'}$ refer to the effective qubit state. It should be noted that equation 24 shows that the two effective qubits which are closest to the defect are slightly entangled. This is attributed to the left pentagon operator, located below and caused by the defect, that slightly entangles them. We then apply the $O(t = T)$ to get new basis:

$$|00\rangle_{t=T} = |00\rangle(|0\rangle + |1\rangle) \quad (30)$$

$$|01\rangle_{t=T} = |00\rangle(|0\rangle - |1\rangle) \quad (31)$$

$$|10\rangle_{t=T} = |00\rangle(|0\rangle + |1\rangle) \quad (32)$$

$$|11\rangle_{t=T} = |00\rangle(|0\rangle - |1\rangle) \quad (33)$$

$$(34)$$

These are correct basis of S_c at $t = T$. operators unchanged! Notice the aforementioned entanglement is removed since the defect is moved away. Consequently, can freely move the defect at this phase! We are then able to demonstrate the process of creation and fusion in the same context. However, we present this in a clearer manner. Consider the state of the original Hamiltonian¹⁶. The state is simultaneously the ground state of Stabilizer center S_c and the ground state of each plaquette term W_p . Assuming we have a time-varying Hamiltonian $H(t)$:

$$H(t) = -H(0)(1 - \frac{t}{T}) - H(T)\frac{t}{T} \quad (35)$$

If we have both $H(0)$ and $H(T)$, representing the dominant coefficients of $S_c(0)$ and $S_c(T)$, the time evolution operator of the form 20 would commute with all the plaquette terms. Which means if we start with the ground state of $S_c(0)$, with form 29, we would reach at

$$|GS\rangle_{t=T} = \Pi_{p \in P} \frac{B_p + 1}{2} \left\{ O(T) \bigotimes_{v \in V'} |0\rangle \right\} \quad (36)$$

The ground state of all plaquette terms remains unchanged. Therefore, it is crucial to consider the time-evolution action on a specific initial product state of $S_c(0)$. We expect the state will transition into the spectrum of new stabilizer centers. Now, it is adequate to focus on one chain as depicted in figure 10. In this figure, we assign red edges to the check operator $X \otimes X$, and the blue edges to $Z \otimes Z$. Furthermore, we denote these operators by Op_i , where i represents the number assigned to the edges. Initially, all blue checks are selected to be the Stabilizer center. We present some vital processes via this platform. The first involves the creation of defects through the implementation of the following Hamiltonian:

$$H(t) = -(Op_1 + Op_3)(1 - \frac{t}{T}) - (Op_2) \frac{t}{T} \quad (37)$$

We erase those terms that commute with $H(t)$. Numerical solution shows, the time evolution operator is given by:

$$O^{creation}(T) = \beta(T)(1 + Op_2) \quad (38)$$

Which means the state would be projected to the ground state of Op_2 , as expected. This results in the creation of a pair of defects, as illustrated in the transition from figure 8a to figure 8b. In the second scenario, one of the defects is moved. This can be achieved through the following process:

$$H(t) = -(Op_2 + Op_5)(1 - \frac{t}{T}) - (Op_2 + Op_4) \frac{t}{T} \quad (39)$$

As shown explicitly above, this time evolution is as expected. The final process under consideration is the fusion process. The first fusion case is that a pair of defects is created and subsequently fused back. This process is essentially the reverse of creation.

$$H(t) = -Op_2(1 - \frac{t}{T}) - (Op_1 + Op_3) \frac{t}{T} \quad (40)$$

The corresponding numerical solution of the time evolution operator is as follows:

$$O(T) = \beta_3(T)(1 + Op_1)(1 + Op_3) + \beta_4(T)[(1 - Op_1)(1 + Op_3) + (1 + Op_1)(1 - Op_3)] \quad (41)$$

In this scenario, only $(1 + Op_1)(1 + Op_3)$ contributes non-zero values, a fact that can be confirmed by examining energy levels. This suggests that after fusing the

pair, we regain the vacuum state as anticipated algebraically. Another fusion case is that we create two pairs of defects from the vacuum, as depicted in figure 8d, and fuse the two central defects. Let us denote the state before fusion as $|GS_4\rangle$, which is derived by creating four defects from $|GS\rangle$ as seen in 29. The subsequent process transforms these two pairs into a single pair:

$$H(t) = -Op_5(1 - \frac{t}{T}) - (Op_4 + Op_6)\frac{t}{T} \quad (42)$$

The TEO is similar as 3.4:

$$O(T) = \beta_5(T)(1+Op_4)(1+Op_6) + \beta_6(T)[(1-Op_4)(1+Op_6) + (1+Op_4)(1-Op_6)] \quad (43)$$

Normalization of the projectors need not be a concern, since $\langle GS_4|(1 \pm Op_4)(1 \pm Op_6)|GS\rangle$ is consistently identical. To understand this, notice that:

$$\langle GS_4|Op_4(Op_6)|GS_4\rangle = 0 \quad (44)$$

This is because $Op_4(Op_6)|GS_4\rangle$ has different energy from $|GS\rangle$. The intricate part is:

$$\langle GS_4|Op_4 \otimes Op_6|GS\rangle = \left(\bigotimes_{v' \in V} \langle 0|_{v'} \right) \Pi_{P \in P} \frac{W_P + 1}{2} Op_4 \otimes Op_6 \left(\bigotimes_{v'' \in V'} |0\rangle_{v''} \right) \quad (45)$$

Notice:

$$\left(\bigotimes_{v' \in V'} \langle 0|_{v'} \right) \Pi_{P \in P'} W_P Op_4 \otimes Op_6 \left(\bigotimes_{v'' \in V'} |0\rangle_{v''} \right) = 0 \quad (46)$$

Because, for any $P' \subset P$, the product of W_P s always form a trivial loop of the lattice, which can not match the action of the four qubit operator $Op_4 \otimes Op_6$.

Naturally, $(1+Op_4)(1+Op_6)$ yields the vacuum, while $(1-Op_4)(1+Op_6) + (1+Op_4)(1-Op_6)$ gives rise to a free fermion. The coefficients of these two outcomes are dictated by the fusion rule of the Ising Anyon:

$$\beta_5(T) = \sqrt{2}\beta_6(T) \quad (47)$$

Numerical solutions suggest that $|\beta_5(T)| = \sqrt{2}|\beta_6(T)|$, with a surprisingly introduced phase. However, we can account for this by incorporating the phase into the definition of the state. As highlighted in [5], the free fermion excitation exhibits the same algebra as the composite quasi-particle of electric and magnetic charge ϵ of the toric code, even though they differ in energy. Kitaev proposed that the free fermion would decay to ϵ when exposed to a certain thermal bath. Consequently, we can deduce that the defects explicitly comply with the nontrivial fusion rule of the Ising Anyon as demonstrated in [3]:

$$\sigma \times \sigma = 1 + \epsilon \quad (48)$$

σ represents the twist defect. ϵ represents the fermion.

Remark: We argue it is free fermion excitation in that it violates check operator but no the plaquette operator. It could only be a fermion in the language of majarona representation.

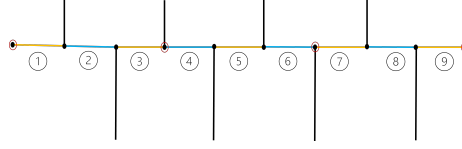


Figure 10: The image displays a local section of the lattice, where alternating red and blue edges represent the $X \otimes X$ and $Z \otimes Z$ checks respectively. Each edge is labeled by a unique number, with the check operator of the corresponding edge identified accordingly. The red circles indicate the positions intended for defect placement.

3.4.1 Possible Measurement-Based initializing method

We have emphasized that since each process is described by time evolution, which is natural to depict each process (movement, creation and fusion) by quantum circuit. Here we put down a convenient measurement-based method to initialize a ground state of the effective toric code on a honeycomb lattice as in figure 11, which is actually the same way as in the Floquet code in [14]. The method is to follow a measurement schedule:

- Step 1: Measure the check operators associated with yellow edges.
- Step 2: Measure the check operators associated with blue edges.
- Step 3: Measure the check operators associated with red edges.
- Step 4: repeat step 1.

After step 4, the state is the ground state of all plaquette terms (with signs that depend on measurement outcomes). We then proceed to measure the yellow checks (or equivalently the elements in S_c) as depicted in fig 6. Following this measurement, the state would transition into the ground state of the plaquette operators and the stabilizer center S_c (still the corresponding eigenvalues depend on the measurement outcome), thereby generating the effective toric code we want. Then we can apply the unitary operator which is given by the time evolution operators in previous section, to manipulate the twist defects.

3.5 Subsystem Code aspects

In recent work of [16], the Kitaev spin liquid code on trivalent and 3-colorable lattice has been proved to be a zero-logical-qubit subsystem code. Here we generalize it to our case. We use some notations to describe the lattice by n_v , the number of vertices, n_e , the number of edges, n_p , the number of plaquettes. We only look at orientable lattice, which could be easily extended to non-orientable cases. We would first prove it is true when all the vertices of lattice have odd degrees. The gauge group is generated by $P_e | e \in E$. So the number of gauge group generators is $n_e - 1$ due to the $\prod_{e \in E} P_e = 1$. Then the generators of stabilizer group S is generated by $\{W_p | p \in P\} \cup \{P_l\}$ where the set P_l refer to the product of check operators along non-trivial loops of the lattice. So the number of the generators of S is given by $n_p - 1 + k$, where k is the number of

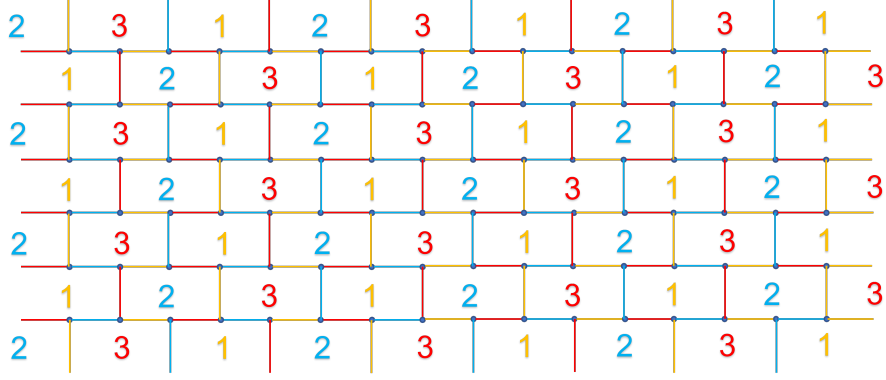


Figure 11: This figure illustrates a honeycomb lattice used to initialize a ground state of the effective toric code, a platform that facilitates defect manipulation. Each edge is colored according to the plaquettes to which it is connected.

non-trivial loop on the lattice. Assume vertex v has degree d_v and t_v qubits are placed on it. Then:

$$n_v - n_e + n_p = 2 - k \quad (49)$$

$$2n_e = \sum_v d_v \quad (50)$$

$$n_q = \sum_v t_v \quad (51)$$

Where n_q is the number of total qubits. The number of logical qubit n_L of this subsystem code is given by

$$n_L = n_q - (n_g - n_s)/2 - n_s \quad (52)$$

$$= 1/2 (2n_q - n_g - n_s) \quad (53)$$

$$= 1/2 (2n_q - n_e - n_p + 2 - k) \quad (54)$$

$$= 1/2 (2n_1 - n_e + n_v - n_e) \quad (55)$$

$$= 1/2 (\sum_{v \in V} 2t_v + 1 - d_v) \quad (56)$$

In our setup, the number of qubit on an odd degree vertex is given by $t_v = (d_v - 1)/2$. So it will automatically let $n_L = 0$. An even degree vertex could be treated as two connected odd degree vertices as depicted in Fig. 5, but in a converse manner. Clearly, this splitting does not change any of the aforementioned total quantities. So our generalized two dimensional Kitaev spin model is always a zero-logical-qubit subsystem.

4 Conclusion and outlook

In this paper, we have generalized the Kitaev spin liquid model on a general planar lattice. We proposed that if we can identify a stabilizer center S_c to satisfy certain requirement, that S_c contains maximum amount of commuting check operators, the vicinity of the ground state will be effectively toric code model. If a single trivalent vertex remains in the shrunk lattice, a twist defect would emerge, exhibiting Non-Abelian statistics as an Ising Anyon. We have conclusively shown that we can manipulate and fuse the defect as long as the Hamiltonian is altered slowly. Furthermore, the processes of creation, movement, and fusion are all governed by the time evolution operator, which are inherently unitary operators. Nonetheless, braiding continues to pose a challenge in this context. In conclusion, we can always recover a surface code with defects, or holes under proper choice of a Stabilizer Center S_c . The generalized spin liquid model appears to be a versatile platform for realizing a general surface code.

Several promising directions for future research emerge from this study. For instance, the nature of a defect resulting from a left vertex of degree 5 remains to be explored. An extension into three dimensions would also be an intriguing prospect, and is currently under preparation. Moreover, a more general and analogous generalization that could support the non-Abelian Kitaev Quantum Double model would be of significant interest and importance.

Acknowledgments.

The authors are partially supported by NSF CCF 2006667, Quantum Science Center (led by ORNL), and ARO MURI.

References

- [1] A. Yu Kitaev. “Fault-tolerant quantum computation by anyons”. In: *Annals of Physics* 303.1 (Jan. 2003). arXiv:quant-ph/9707021, pp. 2–30. DOI: 10.1016/S0003-4916(02)00018-0.
- [2] Michael A. Levin and Xiao-Gang Wen. “String-net condensation: A physical mechanism for topological phases”. In: *Physical Review B* 71.4 (Jan. 2005), p. 045110. DOI: 10.1103/PhysRevB.71.045110.
- [3] H. Bombin. “Topological Order with a Twist: Ising Anyons from an Abelian Model”. In: *Physical Review Letters* 105.3 (July 2010). arXiv:1004.1838 [cond-mat, physics:hep-th, physics:quant-ph], p. 030403. DOI: 10.1103/PhysRevLett.105.030403.
- [4] T. I. Andersen et al. “Non-Abelian braiding of graph vertices in a superconducting processor”. In: *Nature* (May 11, 2023). ISSN: 1476-4687. DOI: 10.1038/s41586-023-05954-4. URL: <https://doi.org/10.1038/s41586-023-05954-4>.

- [5] Alexei Kitaev. “Anyons in an exactly solved model and beyond”. In: *Annals of Physics* 321.1 (Jan. 2006). arXiv:cond-mat/0506438, pp. 2–111. DOI: 10.1016/j.aop.2005.10.005.
- [6] Huaixiu Zheng, Arpit Dua, and Liang Jiang. “Demonstrating non-Abelian statistics of Majorana fermions using twist defects”. In: *Physical Review B* 92.24 (Dec. 2015), p. 245139. DOI: 10.1103/PhysRevB.92.245139.
- [7] Yi-Zhuang You and Xiao-Gang Wen. “Projective non-Abelian Statistics of Dislocation Defects in a Z_N Rotor Model”. In: *Physical Review B* 86.16 (Oct. 2012). arXiv:1204.0113 [cond-mat, physics:quant-ph], p. 161107. DOI: 10.1103/PhysRevB.86.161107.
- [8] Victor Chua, Hong Yao, and Gregory A. Fiete. “Exact chiral spin liquid with stable spin Fermi surface on the kagome lattice”. In: *Physical Review B* 83.18 (May 2011), p. 180412. DOI: 10.1103/PhysRevB.83.180412.
- [9] Congjun Wu, Daniel Arovas, and Hsiang-Hsuan Hung. “ Γ -matrix generalization of the Kitaev model”. In: *Physical Review B* 79.13 (Apr. 2009), p. 134427. DOI: 10.1103/PhysRevB.79.134427.
- [10] Hong Yao, Shou-Cheng Zhang, and Steven A. Kivelson. “Algebraic spin liquid in an exactly solvable spin model”. In: *Physical Review Letters* 102.21 (May 2009). arXiv:0810.5347 [cond-mat], p. 217202. DOI: 10.1103/PhysRevLett.102.217202.
- [11] Gino Cassella et al. “An Exact Chiral Amorphous Spin Liquid”. In: (Aug. 2022). arXiv:2208.08246 [cond-mat]. URL: <http://arxiv.org/abs/2208.08246>.
- [12] Shinsei Ryu. “Three-dimensional topological phase on the diamond lattice”. In: *Physical Review B* 79.7 (Feb. 2009). arXiv:0811.2036 [cond-mat], p. 075124. DOI: 10.1103/PhysRevB.79.075124.
- [13] Tim Eschmann et al. “Thermodynamic classification of three-dimensional Kitaev spin liquids”. In: *Physical Review B* 102.7 (Aug. 2020). arXiv:2006.07386 [cond-mat], p. 075125. DOI: 10.1103/PhysRevB.102.075125.
- [14] Matthew B. Hastings and Jeongwan Haah. “Dynamically Generated Logical Qubits”. In: *Quantum* 5 (Oct. 2021). arXiv:2107.02194 [quant-ph], p. 564. DOI: 10.22331/q-2021-10-19-564.
- [15] Olga Petrova, Paula Mellado, and Oleg Tchernyshyov. “Unpaired Majorana modes on dislocations and string defects in Kitaev’s honeycomb model”. In: *Phys. Rev. B* 90 (13 Oct. 2014), p. 134404. DOI: 10.1103/PhysRevB.90.134404. URL: <https://link.aps.org/doi/10.1103/PhysRevB.90.134404>.
- [16] Christophe Vuillot. “Planar Floquet Codes”. In: arXiv:2110.05348 (Dec. 2021). arXiv:2110.05348 [quant-ph]. URL: <http://arxiv.org/abs/2110.05348>.

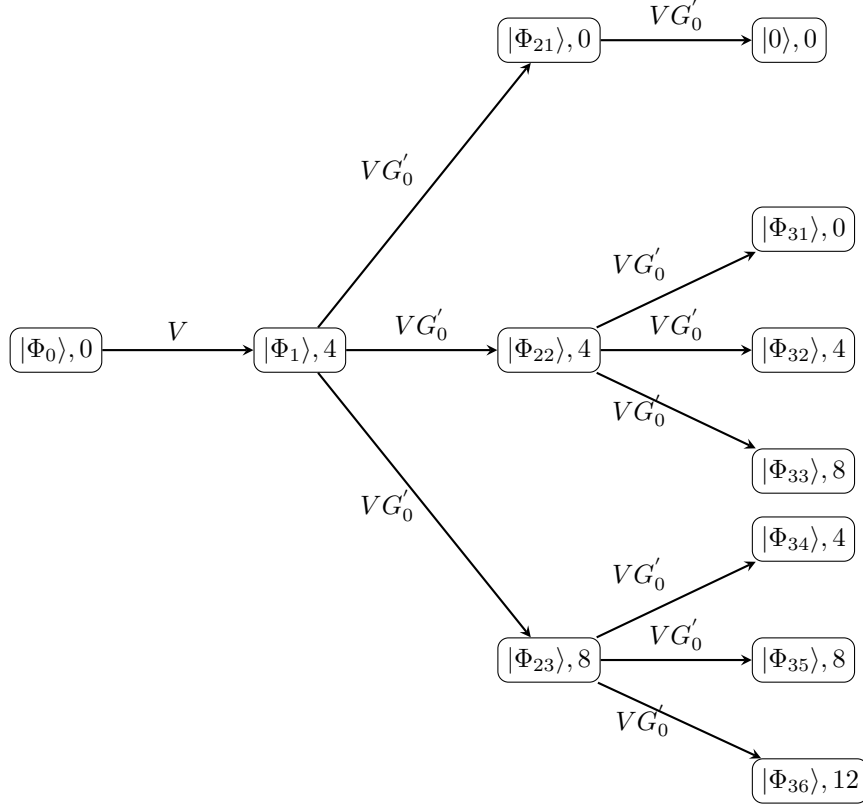


Figure 12: Demonstration of perturbation theory

A Perturbation treatment

For the effective Hamiltonian as follows:

$$H_{eff} = T(V + VG'_0V + VG'_0VG'_0V + \dots)T \quad (57)$$

Where, $T = |GS\rangle\langle GS|$ is the projector onto the ground state of J_v s, and $G'_0 = (1/(E_0 - H_0))'$, where the prime notation implies G'_0 vanishes on the ground state and acts normally on the excited states.

Let's consider the actions of the perturbed terms. As we are examining a general lattice without translational symmetry, we will only track the order of λ for each term.

Each node of the diagram is labeled with a state Φ . The action of each check operator on $|\Phi_0\rangle = |GS\rangle$ will flip two P_v s, which increases the energy by 4. Then, when we apply another V on the resulting state $|\Phi_1\rangle$, different outcomes appear due to the product of $P_{e_1} \times P_{e_2}$, where:

If $\partial e_1 \cap \partial e_2 = \emptyset$, then we obtain $|\Phi_{23}\rangle$ with energy 8. If $\partial e_1 = \partial e_2$, then we obtain $|\Phi_{21}\rangle$, which reverts back to the ground state. The remaining possibility

is that e_1 and e_2 share one common vertex and will have energy 4. If we repeat this process to achieve higher order perturbation, we obtain different sectors with different energy levels as shown in Figure 12. The energy sector $\Phi_{i,j}$ that reverts back to the ground state will contribute to the i th order of the effective Hamiltonian. Note that in the diagram, G'_0 always gives some constant factor. Thus, we conclude:

$$H_{eff}^i = \alpha_i \langle GS | V^i | GS \rangle \quad (58)$$

Where α_i is a path-dependent factor calculable from the diagram. Here, we can neglect this factor, focusing only on the order of λ . Note that terms in V^i that do not vanish in the ground state are those that commute with all P_v . Generators could be $P_{e_i} P_{e_j}$, where $e_i = e_j$, contributing to a constant factor, or $\Pi_{e_j} P_{e_j}$, where e_j forms a closed loop, contributing to the plaquette term $W_p = \Pi_{e \in Bo(p)} P_e$. General terms are possible products of the generators mentioned above. Then we could conclude, the effective Hamiltonian is:

$$H_{eff} = \sum_p \alpha_{l_p} \lambda^{l_p} W_p + constant \quad (59)$$

Where l_p is the number of elements in $Bo(p)$. The factor of $\alpha_{l_p} \lambda^{l_p}$ arises because the dominant contribution of W_p will appear in the l_p order perturbation.

Remark: In a general lattice with $d_v = 4$, we should note that the coefficient of each W_p is no longer uniform. Let's continuously deform the coefficients of W_p s to be uniformly large, regardless of the sign (as we have argued, the sign does not matter in the toric code Model). Notice that this is a continuous transformation which does not close the gap. Therefore, it will stay in the same phase.

B Mapping Table of vertex with $d_v > 4$

Consider a vertex has degree $d_v > 4$. Let us assume $d_v = 2k$, so there are k qubits placed on it. We call an operator a k -order Pauli operator if it is a tensor product of k Pauli operators. We insist choosing $P_v = \bigotimes_k Z$, since the k qubits would stay on the ground state of P_v , with eigenstate of $+1$, without loss of generality, the eigenspace would be 2^{k-1} dimensional. So we have to find the effective $k-1$ order Pauli operators of those k order Pauli operators commuting with P_v . The generators of these k order are of following form:

$$\mathcal{X}_i = \underbrace{1 \otimes 1 \cdots 1}_{i-1} \otimes X \otimes X \otimes 1 \otimes \cdots 1 \otimes 1 \quad (60)$$

Here \mathcal{X} represents a tensor product of k pauli operator. \mathcal{X}_i is explicitly two X operator at position i and $i+1$, identity 1 at the others. We have obviously $k-1$ such operator $\{\mathcal{X}_i | i = 1, 2 \dots k-1\}$. Another set of generators are:

$$\mathcal{Z}_i = \underbrace{1 \otimes 1 \cdots 1}_{i-1} \otimes Z \otimes 1 \cdots 1 \otimes 1 \quad (61)$$

Which means \mathcal{Z}_i is one Z operator locates at position i , Identity 1 at the others. We have k such operators, $\{\mathcal{Z}_i|i = 1, 2, \dots, k\}$. Notice, $|\phi_0\rangle = \bigotimes_k |0\rangle$ is one of the basis in the eigenspace. $\mathcal{X}_i|\phi_0\rangle$ effectively generate the whole eigenspace. Then we define the mapping of \mathcal{X}_i to $k-1$ order operator:

$$\mathcal{X}_i \rightarrow \underbrace{1 \otimes 1 \cdots 1}_{i-1} \otimes X \otimes X \otimes 1 \otimes \cdots 1 \otimes 1 \quad (62)$$

We denote the notation $\tilde{\mathcal{X}}_i$ to represent the effective action of \mathcal{X}_i in the eigenspace of P_v . Notice on the right, it is a tensor product of $k-1$ Pauli operators. Similarly, $\tilde{\mathcal{Z}}_i$ to represent the effective operator of \mathcal{Z}_i :

$$\tilde{\mathcal{Z}}_i = \underbrace{1 \otimes 1 \cdots 1}_{i-2} \otimes Z \otimes Z \otimes 1 \otimes \cdots 1 \otimes 1 \quad (63)$$

For $1 < i < k-1$, and $\tilde{\mathcal{Z}}_1 = Z \otimes 1 \cdots 1 \otimes 1$, $\tilde{\mathcal{Z}}_k = 1 \otimes 1 \cdots 1 \otimes Z$. Notice the product of $\tilde{\mathcal{Z}}_i$ is 1, which agree with $\prod_{i=1}^k \mathcal{Z}_i = P_v$. Then arranging the operators similarly as in 4b would give rise to the splitting of $d_v > 6$.